Princeton Plasma Physics Laboratory

PPPL-5149

Heat flux viscosity in collisional magnetized plasmas

C. Liu, W. Fox, and A. Bhattacharjee

July 2015

Prepared for the U.S. Department of Energy under Contract DE-AC02-09CH11466.

Princeton Plasma Physics Laboratory
Report Disclaimers

Full Legal Disclaimer

This report was prepared as an account of work sponsored by an agency of the United States Government. Neither the United States Government nor any agency thereof, nor any of their employees, nor any of their contractors, subcontractors or their employees, makes any warranty, express or implied, or assumes any legal liability or responsibility for the accuracy, completeness, or any third party's use or the results of such use of any information, apparatus, product, or process disclosed, or represents that its use would not infringe privately owned rights. Reference herein to any specific commercial product, process, or service by trade name, trademark, manufacturer, or otherwise, does not necessarily constitute or imply its endorsement, recommendation, or favoring by the United States Government or any agency thereof or its contractors or subcontractors. The views and opinions of authors expressed herein do not necessarily state or reflect those of the United States Government or any agency thereof.

Trademark Disclaimer

Reference herein to any specific commercial product, process, or service by trade name, trademark, manufacturer, or otherwise, does not necessarily constitute or imply its endorsement, recommendation, or favoring by the United States Government or any agency thereof or its contractors or subcontractors.

PPPL Report Availability

Princeton Plasma Physics Laboratory:

http://www.pppl.gov/techreports.cfm

Office of Scientific and Technical Information (OSTI):

http://www.osti.gov/scitech/

Related Links:

U.S. Department of Energy

U.S. Department of Energy Office of Science

U.S. Department of Energy Office of Fusion Energy Sciences

Heat flux viscosity in collisional magnetized plasmas

C. Liu,[1, a)] W. Fox,[2] and A. Bhattacharjee[1, 2]

[1)] *Princeton University, Princeton, New Jersey 08544, USA*

[2)] *Princeton Plasma Physics Laboratory, Princeton, NJ 08543, USA*

(Dated: 5 April 2015)

Momentum transport in collisional magnetized plasmas due to gradients in the heat flux, a "heat flux viscosity", is demonstrated. Even though no net particle flux is associated with a heat flux, in a plasma there can still be momentum transport owing to the velocity dependence of the Coulomb collision frequency, analogous to the thermal force. This heat-flux viscosity may play an important role in numerous plasma environments, in particular in strongly-driven high-energy-density plasma, where strong heat flux can dominate over ordinary plasma flows. The heat flux viscosity can influence the dynamics of the magnetic field in plasmas through the generalized Ohm's law, and may therefore play an important role as a dissipation mechanism allowing magnetic field line reconnection. The heat flux viscosity is calculated directly using the finite-difference method of E. M. Epperlein and M. G. Haines [M. G. Haines, Phys. Fluids 29, 1029 (1986)], which is shown to be more accurate than S. I. Braginskii's method [S. I. Braginskii, Rev. Plasma Phys. 1, 205 (1965)], and confirmed with one-dimensional collisional particle-in-cell simulations. The resulting transport coefficients are tabulated for ease of application.

[a)] Electronic mail: cliu@pppl.gov

I. INTRODUCTION

Recent experiments and theory have demonstrated the interesting interplay between magnetic fields and heat flux in plasmas. In particular, in high-energy-density plasmas, strong magnetic fields, whether self-generated or externally applied, can be advected by the extreme heat fluxes associated with strong localized heating from lasers or currents. Even at high plasma beta, where the fields may not be expected to play a dominant global energetic role, narrow regions can arise with highly compressed fields altering force balance, and the fields can magnetize electrons and inhibit cross-field transport. For example, magnetized implosions on OMEGA have demonstrated improvement in fusion performance with externally applied fields of order 10 T, subsequently compressed to 1000's of T[1]. Self-generated magnetic fields may also play roles in controlling the heat transport in coronal plasmas[2] and in ICF hohlraums[3].

The interesting new effect in these semi-collisional plasmas is that the heat flux itself can push magnetic fields around, resulting from the Nernst effect[4]. This effect results from the well-known v^{-3} velocity dependence of the collision frequency in plasmas. Intuitively, the Nernst effect results if one considers the electron population to be divided into "hot" and "cold" populations, so that the magnetic fields are frozen to the weakly-collisional hot population but diffuse with respect to the cold plasma, and more specifically, across the compensating cold return current. The Nernst effect has received some experimental observations in laser-produced plasmas, namely observation of extremely fast advection of self-generated magnetic fields away from a laser focal spot[9,10]. On the theoretical front, the Nernst effect leads to a number of effects controlling the magnitude of magnetic fields generated during laser-plasma interaction, including compressive amplification of magnetic fields in ablation fronts[5–8] or conversely, saturation of self-generated magnetic fields by outward Nernst convection[11]. Finally, recent simulations including multiple laser-produced plasma plumes have shown that the Nernst effect can drive magnetic reconnection of the self-generated magnetic fields.[12].

These results call for a detailed theoretical understanding of the role of the heat-flux on magnetic fields in such plasmas. The evolution of the magnetic field is ultimately derived from Faraday's law in association with the generalized Ohm's law, which in HED plasma

conditions may be written schematically as[4],

$$\boldsymbol{E} + \frac{\boldsymbol{v} \times \boldsymbol{B}}{c} - A_H \frac{\boldsymbol{j} \times \boldsymbol{B}}{n_e e c} + A_N \frac{\boldsymbol{Q}_e \times \boldsymbol{B}}{p_e} = \eta_{\parallel} \boldsymbol{j}_{\parallel} + \eta_{\perp} \boldsymbol{j}_{\perp} - \frac{\nabla \cdot \mathbf{P}_e}{n_e e} - \mathbf{A_T} \cdot \nabla T_e. \qquad (1)$$

Here the terms on the left-hand-side (LHS) of Eq. (1) represent respectively, the electric field, advection by bulk plasma flow, the Hall term, and advection by heat flux (the Nernst effect). (The pre-factors A_H, A_N represent collisional corrections to these terms, for example as calculated by Haines (1986)[4]). Terms on the right-hand-side (RHS) include possible dissipation mechanisms, including plasma resistivity with the well-known anisotropy parallel and perpendicular to magnetic field, the electron pressure tensor $\mathbf{P}_e$, and the thermoelectric effect. The pressure tensor includes electron viscosity effects.

While typically not important in determining the bulk flow, the dissipation terms are extremely important in the narrow current layers formed by reconnection or shocks. In magnetic reconnection current sheets, the external drive terms (which in this case can include a Nernst-effect drive) break down and non-ideal dissipative terms must take over to allow reconnection[13]. These non-ideal terms can result from resistivity or off-diagonal terms in the pressure tensor (stress tensor), which embodies both electron kinetic effects in the current sheet in collisionless regimes[14,15], and also momentum transport resulting from electron viscosity (resulting in hyper-resistivity)[16]. Indeed in the results from Joglekar et al (2014), which studied reconnection in heat-flux-driven regimes, it was found that reconnection in the reconnection layer was supported by the pressure tensor[12]. The pressure tensor was calculated from first principles within a Vlasov-Fokker-Planck code, but the ultimate origins were not studied.

In this paper, we demonstrate momentum transport originating from gradients in heat flux, a "heat flux viscosity," through solution to the kinetic equation. Even though there is no net particle flow associated with a heat flux, the heat-flux viscosity still exists due to the velocity dependence of the collision frequency, analogous to the thermal force. Interestingly, we find that some components of the heat-flux viscosity tensor can change sign with collisionality; this is shown to result from the variation of the momentum diffusivity with particle energy, from magnetized to unmagnetized energy regimes. We calculate both the standard flow viscosity and the heat flux viscosity from solution to the kinetic equation, using the finite-difference method of Epperlein and Haines[17], thus generalizing their results. The finite-difference-method is found to be more accurate than Braginskii's lowest-order

polynomial method, which apparently does not capture accurately the momentum diffusivity in different regions of momentum space. Instead, good results are obtained with direct numerical solution of the kinetic equation with the finite difference method. Finally, Tte results obtained by finite-difference-methods are finally confirmed independently with 1-D collisional particle-in-cell simulations.

II. HEAT-FLUX VISCOSITY CALCULATION

We now calculate the heat-flux viscosity effect from the kinetic equation. We follow standard techniques appropriate for collisional plasmas, assuming an expansion of the distribution function in the parameter ϵ, the ratio of mean free path to gradient scale length, assumed to be much smaller than 1. For a comprehensive collision operator such as the Landau operator, the expanded kinetic equations become a set of integrodifferential equations. To subsequently solve these equations, various polynomial expansion methods have been introduced, including the Laguerre polynomials of Braginskii[18], or Hermite polynomials[19].

In the 1980s, Epperlein and Haines[17,20] showed that some of Braginskii's transport coefficients can exhibit large inaccuracies in certain ranges of $\Omega\tau$ (Ω is the electron gyrofrequency and τ is the collision time) and incorrect asymptotic behaviors, because in Braginskii's work only the first two terms of the Laguerre polynomial expansion were kept. (We refer to this method hereafter by LPE2). Epperlein and Haines then developed a finite difference method (hereafter FDM) to numerically solve the kinetic equation[17]. Their method gave more accurate results and more importantly, demonstrated the correct asymptotic behavior for the transport coefficients. For ease of use, they used rational polynomials to numerically fit the results, resulting in transport coefficient which had similar form to Braginskii's but with fractional error less than 15%. Most recently, Ji and Held[21] re-examined the Braginskii method, and showed that Laguerre polynomial expansion method can in fact have good agreement with the finite difference method by including very high orders of polynomials (up to 160 in their paper). However, for a small number of polynomials it appears impossible to obtain the correct asymptotic behavior.

In this work we calculate both the particle flow viscosity (PFV) and heat-flux viscosity (HFV) using the FDM method of Epperlein and Haines[17]. (In their work, Epperlein and Haines calculated the first-order fluxes $(\mathbf{j}, \mathbf{q_e})$ using the kinetic equation up to first order,

i.e. $\boldsymbol{f}_1$. The viscosity, calculated here, requires the next order kinetic equation for the tensor components $\boldsymbol{f}_2$.) We also compare with a calculation using Braginskii's LPE2 method to make contact with those standard results. Recently, Ji and Held[21] calculated the flow viscosity coefficients using their geometric method, and obtained results in good agreement with (less than 7% deviation) from Braginskii's LPE2 results. We obtain similar agreement.

We then generalize the calculation to the heat-flux viscosity. In contrast to the flow viscosity, we find significant deviations between transport coefficients calculated by LPE2 compared with those calculated by FDM. We show through a simple calculation that these result from errors in the assumed velocity-dependence of the momentum-diffusivity in the LPE2 expansion. In all cases, we express the final transport coefficients in using the same notation as Braginskii[18], but with fractional error less than 5%.

We now proceed with the calculation. Following standard procedure, the electron distribution function f is expanded in a Cartesian form[22],

$$f = f_0 + \boldsymbol{f}_1 \cdot \frac{\boldsymbol{v}}{v} + \boldsymbol{f}_2 : \frac{\boldsymbol{vv}}{v^2} + \cdots . \tag{2}$$

The stress tensor $\boldsymbol{\Pi}$ can be obtained from the integration of $\boldsymbol{f}_2$[23],

$$\boldsymbol{\Pi} = \mathbf{P} - p\mathbf{I}_2 = \frac{8\pi m}{15} \int \boldsymbol{f}_2 v^4 dv. \tag{3}$$

The kinetic equation for $\boldsymbol{f}_2$ is[23]

$$\frac{\partial \boldsymbol{f}_2}{\partial t} + \left(v\nabla \boldsymbol{f}_1 - \frac{v}{3}\mathbf{I}_2 \nabla \cdot \boldsymbol{f}_1 \right) + \left[v\frac{\partial}{\partial v}\frac{\boldsymbol{a}\boldsymbol{f}_1}{v} - \frac{v}{3}\left(\boldsymbol{a} \cdot \frac{\partial}{\partial v}\frac{\boldsymbol{f}_1}{v} \right) \mathbf{I}_2 \right] + 2\boldsymbol{\Omega} \times \boldsymbol{f}_2 + \frac{3}{7} v\nabla \cdot \boldsymbol{f}_3 + \frac{3}{7v^4}\frac{\partial (v^4 \boldsymbol{a} \cdot \boldsymbol{f}_3)}{\partial v} = C_2(\boldsymbol{f}_2), \tag{4}$$

where $\boldsymbol{a}$ is the acceleration force on electrons, $\boldsymbol{\Omega}$ is the electron gyrofrequency in the direction of the magnetic field, and C_2 is the collision operator on $\boldsymbol{f}_2$. For simplicity we focus on electron kinetics and assume the ions are stationary, so we take the the average fluid velocity $\boldsymbol{C}$ to be zero. On the LHS, the second term is the viscosity effect which characterizes the contribution to $\boldsymbol{f}_2$ from gradients of $\boldsymbol{f}_1$. The third term is the combined effect of external forces (e.g. the electric field) and $\boldsymbol{f}_1$. The last two terms are the effects of the higher-order component $\boldsymbol{f}_3$. The term on the RHS is the collision term.

In this paper we focus on the viscosity effect in a steady state in the presence of a magnetic field, so we only keep the second and fourth term on the LHS in Eq. (4). Though

$\boldsymbol{f}_2$ is a traceless symmetric tensor which has 5 degrees of freedom, the two terms are coupled through the term $2\boldsymbol{\Omega}\times\boldsymbol{f}_2$. To decouple the equations, we introduce a complex representation of the tensors in Eq. (4)[23]. Define

$$\mathsf{U} = \frac{v}{2}\left[\nabla\boldsymbol{f}_1 + (\nabla\boldsymbol{f}_1)^T\right] - \frac{v}{3}\mathsf{I}_2\nabla\cdot\boldsymbol{f}_1, \tag{5}$$

which is similar to the strain rate tensor. We then apply the following recombinations

$$f_a = f_{2xx} + f_{2yy} = -f_{2zz}, \qquad U_a = U_{xx} + U_{yy} = -U_{zz}, \tag{6}$$

$$f_b = f_{2yz} + jf_{2xz}, \qquad U_b = U_{yz} + jU_{xz}, \tag{7}$$

$$f_c = f_{2yz} - jf_{2xz}, \qquad U_c = U_{yz} - jU_{xz}, \tag{8}$$

$$f_d = f_{2xx} - f_{2yy} + 2jf_{2xy}, \qquad U_d = U_{xx} - U_{yy} + 2jU_{xy}, \tag{9}$$

$$f_e = f_{2xx} - f_{2yy} - 2jf_{2xy}, \qquad U_e = U_{xx} - U_{yy} - 2jU_{xy}. \tag{10}$$

The kinetic equation then becomes

$$-\eta j\Omega f_n - U_n = C[F_n]. \tag{11}$$

where $\eta = 0, 1, -1, 2, -2$ corresponds to $n = a, b, c, d, e$. This means that there will be different transport coefficients associated with the five components of $\boldsymbol{f}_2$.

The electron collision term consists of the electron-electron and the electron-ion collision operators, $C = C_{ee} + C_{ei}$. We use the following collision terms[23]

$$C_{ee} = n^{-1}\nu_{ee}\left[\frac{v^2}{3}(I_2^0 + J_{-1}^0)\frac{d^2f_2}{dv^2} + \frac{v}{3}(-I_2^0 + 2J_{-1}^0 + 3I_0^0)\frac{df_2}{dv} + (I_2^0 - 2J_{-1}^0 - 3I_0^0)f_2 + 8\pi v^3 f_2 f_0\right.$$
$$\left. + v^2\left[\frac{6}{35}(I_4^2 + J_{-3}^2) - \frac{1}{15}(I_2^2 + J_{-1}^2)\right]\frac{d^2f_0}{dv^2} + v\left[-\frac{6}{35}I_4^2 + \frac{1}{35}J_{-3}^2 + \frac{4}{15}I_2^2 + \frac{1}{15}J_{-1}^2\right]\frac{df_0}{dv}\right], \tag{12}$$

$$C_{ei} = -3\nu_{ei}f_2, \tag{13}$$

where $\nu_{ee} = \left[4\pi n_e(e^2/m_e)^2\ln\Lambda\right]/v^3$, $\nu_{ei} = \left[4\pi n_i(Ze^2/m_e)^2\ln\Lambda\right]/v^3$, and

$$I_j^i = 4\pi v^{-j}\int_0^v f_i v^{2+j}dv, \quad J_j^i = 4\pi v^{-j}\int_v^\infty f_i v^{j+2}dv. \tag{14}$$

Note that there is no difference in the collision term for the five components of $\boldsymbol{f}_2$.

The equations have now been converted to scalar form, and can be solved using the FDM described in Appendix A in Ref. 17. (The same method is also used to solve the kinetic

equation for $\boldsymbol{f}_1$ in this paper.) In other words, for a given tensor $\mathbf{U}$ we obtain a solution of $\boldsymbol{f}_2$, and then calculate the anisotropic pressure components from Eq. (3).

$\boldsymbol{f}_1$ can also be expanded using the generalized Laguerre polynomials[23],

$$f_{1\alpha} = v f_0(W) \sum_r q_{\alpha r} L_r^{3/2}(W), \qquad \alpha = x, y, z \tag{15}$$

$$W = \frac{mv^2}{2T}, \qquad f_0(W) = n \left(\frac{m}{2\pi T}\right)^{3/2} \exp(-W).$$

Using the orthogonality relations of $L_r^{3/2}$, we find that the coefficient q_0 corresponds to the mean particle flow $\boldsymbol{j}$, and q_1 corresponds to the heat flux $\boldsymbol{Q}$,

$$j_\alpha = \frac{4\pi}{3} \int f_{1\alpha} v^3 dv = \frac{nT}{m} q_{\alpha 0}, \tag{16}$$

$$Q_\alpha = \frac{4\pi}{3} \int f_{1\alpha} \left(\frac{mv^2}{2} - \frac{5T}{2}\right) v^3 dv = -\frac{5nT^2}{2m} q_{\alpha 1}. \tag{17}$$

Vice versa, if we apply an $f_{1\alpha}$ which only contains the $L_0^{3/2}$ component to Eq. (11), we can find the off-diagonal pressure components driven by the particle flow, which is the standard flow viscosity. The associated transport coefficients have been calculated by Braginskii[18] using LPE2. If we next apply an $f_{1\alpha}$ with only a $L_1^{3/2}$ component, we find the off-diagonal pressure components driven by the heat flux, from which we can calculate the heat-flux viscosity coefficients.

Here we present the viscosity coefficients for both electron PFV and HFV. For PFV we adopt the same notation as Braginskii[18]. The stress tensor is expressed in terms of the corresponding tensor W and five viscosity coefficients (and without loss of generality we take the magnetic field along the z direction),

$$\Pi_{\alpha\beta} = -\eta_0 W_{0\alpha\beta} - \eta_1 W_{1\alpha\beta} - \eta_2 W_{2\alpha\beta} + \eta_3 W_{3\alpha\beta} + \eta_4 W_{4\alpha\beta}, \quad \alpha, \beta = x, y, z \tag{18}$$

$$W_{0\alpha\beta} = \begin{Bmatrix} \frac{1}{2}(W_{xx}+W_{yy}) & 0 & 0 \\ 0 & \frac{1}{2}(W_{xx}+W_{yy}) & 0 \\ 0 & 0 & W_{zz} \end{Bmatrix},$$

$$W_{1\alpha\beta} = \begin{Bmatrix} \frac{1}{2}(W_{xx}-W_{yy}) & W_{xy} & 0 \\ W_{yx} & \frac{1}{2}(W_{yy}-W_{xx}) & 0 \\ 0 & 0 & 0 \end{Bmatrix}, \quad W_{2\alpha\beta} = \begin{Bmatrix} 0 & 0 & W_{xz} \\ 0 & 0 & W_{yz} \\ W_{zx} & W_{zy} & 0 \end{Bmatrix}, \tag{19}$$

$$W_{3\alpha\beta} = \begin{Bmatrix} -W_{xy} & \frac{1}{2}(W_{xx}-W_{yy}) & 0 \\ \frac{1}{2}(W_{xx}-W_{yy}) & W_{xy} & 0 \\ 0 & 0 & 0 \end{Bmatrix}, \quad W_{4\alpha\beta} = \begin{Bmatrix} 0 & 0 & -W_{yz} \\ 0 & 0 & W_{xz} \\ -W_{zy} & W_{zx} & 0 \end{Bmatrix}.$$

$$W_{\alpha\beta} = \frac{\partial V_\alpha}{\partial \beta} + \frac{\partial V_\beta}{\partial \alpha} - \frac{2}{3}\delta_{\alpha\beta}(\nabla \cdot V). \tag{20}$$

For the HFV, we first define the Nernst velocity[4],

$$\boldsymbol{V}_N = \frac{2}{5}\frac{\boldsymbol{Q}}{n_e T_e}. \tag{21}$$

The HFV then has an analogous set of viscosity coefficients to the PFV model,

$$\Pi^H_{\alpha\beta} = -\mu_0 W^H_{0\alpha\beta} - \mu_1 W^H_{1\alpha\beta} - \mu_2 W^H_{2\alpha\beta} + \mu_3 W^H_{3\alpha\beta} + \mu_4 W^H_{4\alpha\beta}, \quad \alpha,\beta = x,y,z \tag{22}$$

where W^H has the same elements as W in Eq. (19), with the particle velocity replaced by the Nernst velocity,

$$W^H_{\alpha\beta} = \frac{\partial V_{N\alpha}}{\partial \beta} + \frac{\partial V_{N\beta}}{\partial \alpha} - \frac{2}{3}\delta_{\alpha\beta}(\nabla \cdot V_N).$$

Here the coefficients μ_α are all functions of $x = \Omega\tau_e$, where τ_e is the electron collision time $\tau_e = \frac{3}{4}\left(\sqrt{m_e}T_e^{3/2}/\sqrt{2\pi}n_i Z^2 e^4 \ln\Lambda\right)$. We note that the value of μ_0 can be obtained by taking the limit of $x \to 0$ of $\mu_2(x)$, and that $\mu_1 = \mu_2(2x)$ and $\mu_3 = \mu_4(2x)$. Identical relations apply to the coefficients η_α in the PFV. Therefore we only need the coefficients $\eta_2(x)$, $\eta_4(x)$, $\mu_2(x)$ and $\mu_4(x)$, which are calculated using the FDM.

We further define dimensionless transport coefficients, $\mu^c_\alpha = \mu_\alpha/(nT_e\tau_e)$ and $\eta^c_\alpha = \eta_\alpha/(nT_e\tau_e)$. We fit the resulting functions to rational polynomials to obtain the transport coefficients in a form similar to Braginskii. The fitting function we choose is

$$F(x) = \frac{\sum_{j=0}^{n}\alpha_j x^{j+s}}{\left(\sum_{j=0}^{d} a_j x^j\right)^r}. \tag{23}$$

To satisfy the asymptotic behavior obtained from the FDM results, here s is zero for η_2, μ_2, and one for η_4, μ_4, and $r = 1$. To obtain the best fit, we choose to minimize the sum of the square fractional error $\sum [1 - F(x)/\eta^c(x)]^2$. We find that by using $n = 1$ and $d = 3$, compact forms are obtained with the maximal fractional error for every coefficient less than 5% . The polynomial forms are listed below and the polynomial coefficients for different values of ion charge Z are shown in Tables I & II.

$$\eta_2^c = \frac{\alpha_1 x + \alpha_0}{x^3 + a_2 x^2 + a_1 x + a_0}, \quad \eta_4^c = -\frac{x\,(\alpha_1' x + \alpha_0')}{x^3 + a_2' x^2 + a_1' x + a_0'}, \tag{24}$$

$$\mu_2^c = \frac{\beta_1 x + \beta_0}{x^3 + b_2 x^2 + b_1 x + b_0}, \quad \mu_4^c = -\frac{x\,(\beta_1' x + \beta_0')}{x^3 + b_2' x^2 + b_1' x + b_0'}. \tag{25}$$

TABLE I. The fitting coefficients for PFV.

	Z=1	Z=2	Arbitrary Z
η_0^c	0.73349	1.3044	$-1.0543Z^{-4} + 3.5759Z^{-3} - 3.6486Z^{-2} + 0.050576Z^{-1} + 1.8099$
α_0	0.59261	0.28720	$0.035003Z^{-3} + 0.36216Z^{-2} + 0.0056867Z^{-1} + 0.18974$
α_1	2.0810	1.4256	$0.0021329Z^{-3} + 0.87129Z^{-2} + 0.00011515Z^{-1} + 1.2075$
a_0	0.81141	0.22098	$0.53414Z^{-3} + 0.14054Z^{-2} + 0.032489Z^{-1} + 0.10416$
a_1	2.6833	1.0392	$1.0719Z^{-3} + 0.89913Z^{-2} + 0.058879Z^{-1} + 0.65327$
a_2	2.0124	1.8963	$0.23142Z^{-3} - 0.12095Z^{-2} + 0.0082817Z^{-1} + 1.8937$
α_0'	0.092478	0.044457	$-0.013310Z^{-3} + 0.079379Z^{-2} + 0.00020066Z^{-1} + 0.026202$
α_1'	1.0216	1.0207	$-0.0012185Z^{-3} + 0.0025143Z^{-2} + 0.00013602Z^{-1} + 1.0202$
a_0'	0.13097	0.017866	$0.16567Z^{-3} - 0.050613Z^{-2} + 0.011177Z^{-1} + 0.0046967$
a_1'	1.3690	0.37529	$0.82995Z^{-3} + 0.32439Z^{-2} + 0.044833Z^{-1} + 0.16972$
a_2'	0.86899	0.64133	$-0.053373Z^{-3} + 0.36517Z^{-2} + 0.00075059Z^{-1} + 0.55643$

Figure 1 shows the results of the four normalized viscosity coefficients with x ranging from 10^{-2} to 10^2 and the curve of the best-fit polynomials of Eq. (24) and Eq. (25), as well as the results from a separate LPE2 calculation. (The expressions for η_2 and η_4 are directly from Ref. 18.) We can see that for the PFV (η_2 and η_4) LPE2 in fact agrees well with FDM. (This is consistent with the findings of Ref. 21, where it was also found that LPE2 produced good transport coefficients for this viscosity.) However for HFV (μ_2 and μ_4) there is a large

TABLE II. The fitting coefficients for HFV.

	Z=1	Z=2	Arbitrary Z
μ_0^c	1.5080	2.9947	$-4.6410Z^{-4} + 13.533Z^{-3} - 12.089Z^{-2} + 0.18114Z^{-1} + 4.5239$
β_0	6.0388	3.3660	$-0.0920357Z^{-3} + 3.7230Z^{-2} - 0.0652127Z^{-1} + 2.4734$
β_1	-0.43085	-0.57449	$0.020755Z^{-3} + 0.16194Z^{-2} + 0.0068750Z^{-1} - 0.62046$
b_0	3.8611	1.0571	$2.3994Z^{-3} + 0.83225Z^{-2} + 0.11720Z^{-1} + 0.51998$
b_1	2.4339	1.4032	$1.4051Z^{-3} - 0.31397Z^{-2} + 0.071675Z^{-1} + 1.2710$
b_2	2.7209	3.4849	$-0.71780Z^{-3} + 0.021336Z^{-2} - 0.26964Z^{-1} + 3.6880$
β_0'	4.5903	3.2183	$-0.34416Z^{-3} + 2.1972Z^{-2} + 0.045165Z^{-1} + 2.6919$
β_1'	0.98027	0.98295	$0.0021991Z^{-3} - 0.0060078Z^{-2} - 0.00017356Z^{-1} + 0.98425$
b_0'	2.0796	0.34871	$2.3101Z^{-3} - 0.49845Z^{-2} + 0.15305Z^{-1} + 0.1450$
b_1'	1.2464	0.53267	$0.47400Z^{-3} + 0.37693Z^{-2} + 0.030086Z^{-1} + 0.36534$
b_2'	3.4623	2.3921	$-0.28879Z^{-3} + 1.7346Z^{-2} + 0.039201Z^{-1} + 1.9772$

fractional error between LPE2 and FDM over most of the range of x. In particular, we find that μ_2 reverses sign at $x \approx 7.03$ for $Z = 1$, a behavior totally missed by LPE2. One might ask whether this negative transport coefficient might lead to some instability in the fluid equations. However, the coefficients μ_2 and μ_4 are driven by the heat flux gradient rather than particle flow, and correspond to an off-diagonal term in the transport matrix. The negative value of these coefficients does not imply instability in the transport model as long as all the eigenvalues of the matrix are still positive.

The reason that LPE2 gives accurate results for PFV (η_2 and η_4) but inaccurate results for HFV (μ_2 and μ_4) is understood as follows. In the cartesian expansion adopted, viscosity is contained in the second-order distribution function $\boldsymbol{f}_2$, which arises in response to the gradients (shear and compression) of $\boldsymbol{f}_1$. If we apply a delta-function distribution on $\boldsymbol{f}_1$, namely $f_{1\alpha} = \delta(v - v_0)$, then we can obtain the *Green function of the viscosity coefficient*, which is intuitively the momentum diffusivity as a function of velocity,

$$\Theta_n = \int G_n(v_0) f_1(v_0)\, dv_0, \tag{26}$$

where the Θ_n (including real and imaginary parts) correspond to the five components of

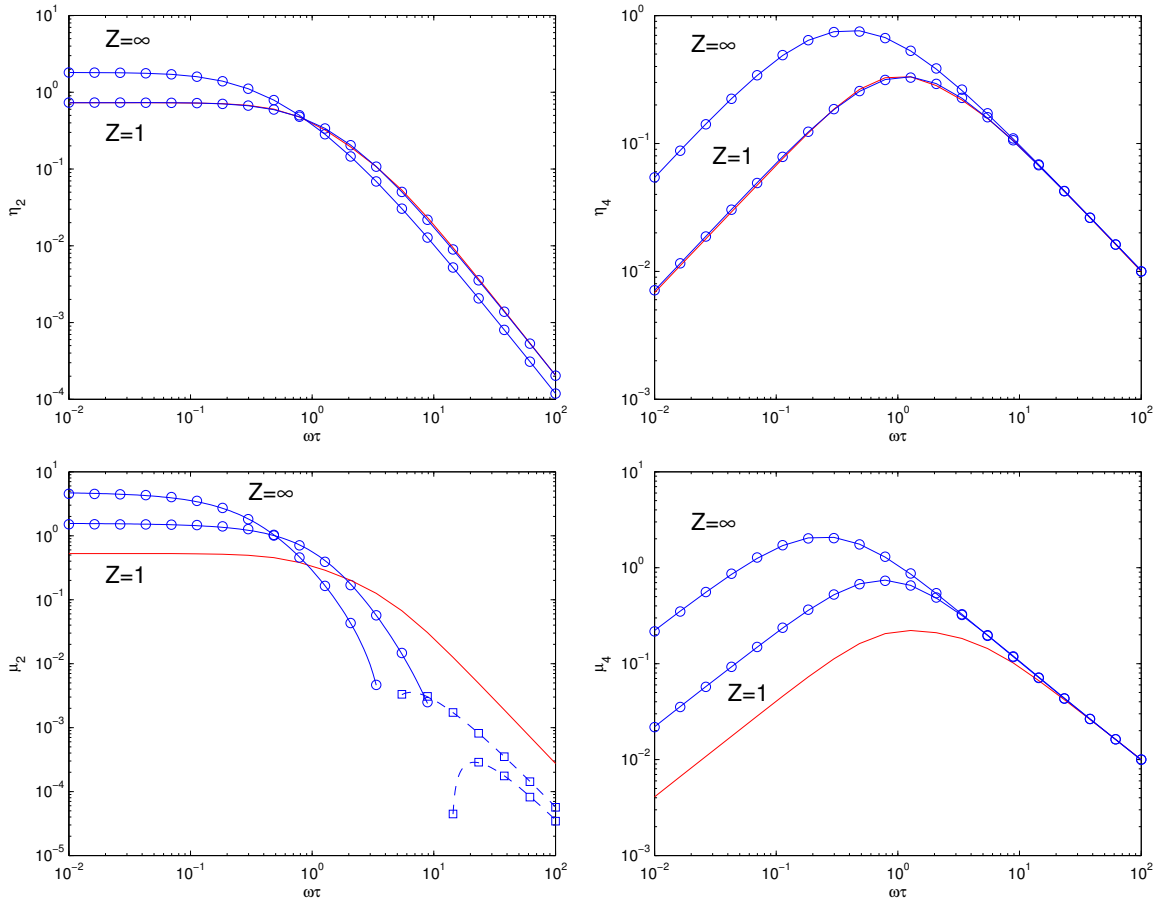

FIG. 1. Viscosity coefficients η_2, η_4, μ_2, μ_4 as functions of $x = \Omega\tau$. The blue circles refer to the FDM results for $Z = 1$ and $Z = \infty$. The blue lines are the fitting polynomial results. The red line is the LPE2 result for $Z = 1$. The dashed lines in the plot of μ_2 correspond to negative value.

viscosity coefficients, and

$$G_n(v_0) = \frac{8\pi m}{15} \int f_n v^4 dv. \tag{27}$$

Here f_n is calculated from Eq (11), with U_n substituted by $v\delta(v - v_0)$. The viscosity for PFV and HFV can then be calculated by applying different forms of f_1 in Eq. (26). Due to the difference in the calculation method, the FDM and LPE2 lead to different forms of the Green function. Fortunately, we can gain insight by using the *Lorentz* collision operator (Eq. (13) in the $Z \to \infty$ limit, in which case the Green function can be calculated analytically. To do so we rewrite the kinetic equation Eq. (11) for $n = b$ as

$$-j\Omega f_b - U_b = -3\nu_{ei} f_b, \tag{28}$$

so that,

$$f_b = \frac{U_b}{3\nu_{ei} - j\Omega}. \tag{29}$$

The real and imaginary parts of f_b correspond to η_2 and η_4 for PFV (or μ_2 and μ_4 for HFV). The asymptotic behavior of the real part of f_b for large v is $f_b \sim 3\nu_{ei}U_b/\Omega^2$. Given that $U_b = v\delta(v - v_0)$ and $\nu_{ei} \sim v^{-3}$, the resulting Green function G_b goes as $\mathrm{Re}[G_b] \sim v_0^2$ for large v.

Figure 2 shows the shape of the real part of Green function (corresponding to η_2 and μ_2) for $\Omega\tau = 10$, $Z = \infty$ (Lorentz plasma) from the analytical calculation, FDM and LPE2. Figure 3 shows the shape of the distribution function f_1 for the case with particle flow (no heat flux), and the case with heat flux (no particle flow).

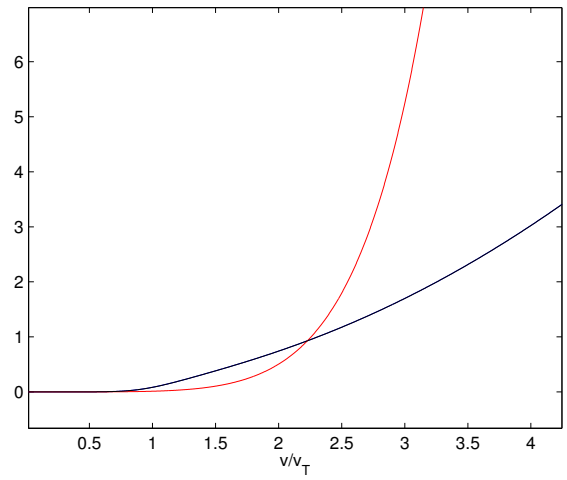

FIG. 2. The real part Green function for Lorentz plasma. The black line is the analytical calculation. The blue line is the result from FDM and the red line is the result from LPE2. Here the blue and black lines overlap.

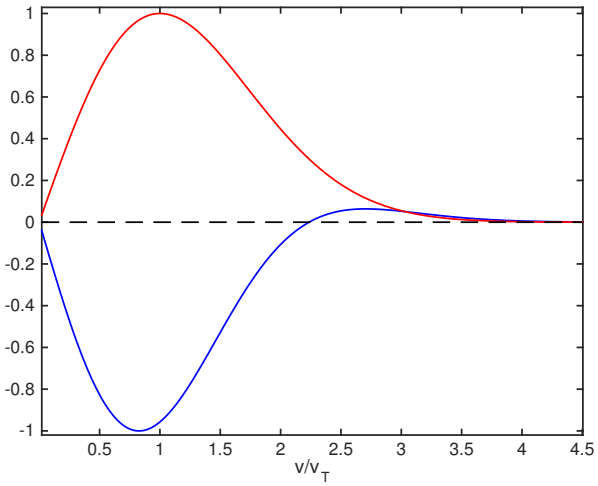

FIG. 3. The distribution function f_1. The dimension is v^{-3}. The red line is the case with particle flow and no heat flux. The blue line is the case with heat flux but no particle flow. Both are normalized with the absolute maximum to be 1.

We can see that the results from FDM and this analytical calculation are almost identical, while LPE2 has incorrect asymptotic behavior. LPE2 misweights the momentum transport in the tails ($v/v_{te} \to 0$ and $\to \infty$). At small velocity, the LPE2 Green function underpredicts momentum transport, but conversely at large velocity it over-predicts momentum transport. This can explain why LPE2 can give good quantitative results for PFV but poor

results for HFV. As shown in Fig. 3, for particle flow the first order distribution function f_1 is always positive, and so the discrepancy between FDM and LPE2 in the low-velocity and high-velocity can compensate to give an agreement between the two. However, for the heat flux viscosity, the distribution f_1 changes signs (as required for no net particle transport), so therefore the resulting momentum transport requires balancing positive and negative momentum transport in the tails. However, the LPE2 Green's function underweights at low-velocity but over-weights at high velocity, both adding to the discrepancy.

III. PARTICLE-IN-CELL SIMULATION

We have tested the results discussed above using a collisional particle-in-cell simulation to directly calculate the electron heat flux viscosity. The simulation adopts a 1D initial condition (varying along z). The plasma is composed of fixed ions and mobile electrons. Initially the electron temperature profile in z has a bump at the center. A magnetic field is applied transverse to the gradient (along x) and is held fixed in space and time. The temperature gradient will drive heat fluxes in the z direction towards the two boundaries and cross-field heat fluxes along the y direction. The resulting gradients of the heat flux will drive off-diagonal terms in the pressure tensor through HFV. Note that in general a temperature gradient will drive both heat flux and particle flow, both of which can generate viscosity. However, in this simulation, the bulk electron flow is prevented by the fixed ions (and the requirement of charge neutrality), so that the heat flux effect dominates here. We use the following parameters: Electron temperature T_e =5keV; case (i) $\Omega = 0.32\omega_{pe}$ and $\Omega\tau = 5$; case (ii) $\Omega = 0.064\omega_{pe}$ and $\Omega\tau = 1$; case (iii) $\Omega = 0.064\omega_{pe}$ and $\Omega\tau_e = 0.2$. We also run a case with zero magnetic field and $\tau_e = 3/\omega_{pe}$. These values are chosen to ensure $\epsilon \ll 1$. The simulation actually employs a 2-D box of size $40d_e \times 80d_e$, and 240×480 cells. In each cell we use 8×10^4 particles to reduce the numerical noise. The simulation is conducted using the PIC code PSC[24].

Fig. 4 shows the off-diagonal pressure component Π_{yz} measured in the simulation for the first 3 cases. We also plot Π_{yz} calculated using the transport coefficients from Eq. (22) and Eq. (25), using the heat flux values measured directly from the simulations. The results using the transport coefficients from LPE2 are also plotted for comparison. We can see that in all three cases the FDM results give good agreement with the PIC simulation results,

while the result from LPE2 gives considerable error. Fig. 5 shows the simulation result for Π_{zz} for the case with zero magnetic field, which again shows that the FDM calculation is more accurate than LPE2.

The sign-change of μ_2 for $\Omega\tau_e \gtrsim 5$ (Fig. 1) is a novel effect so it would be interesting if we could demonstrate its effect in the PIC simulations. However, it turns out that it is difficult to isolate it from other coefficients. Negative μ_2 only occurs in the regime $\omega\tau \gg 1$, where the temperature gradient drives heat flux along both directions perpendicular to the magnetic field. As a result, the components in the anisotropic pressure tensor will be affected not only by μ_1 or μ_2, but also by μ_3 and μ_4. We have found that in the regime that μ_1 or μ_2 is negative, their contribution to the off-diagonal pressure tensor is subdominant compared to that from μ_3 and μ_4. Given that the later does not change sign, the total pressure tensor component does not change sign when μ_2 becomes negative.

IV. CONCLUSIONS

This work has demonstrated for the first time a heat flux viscosity effect—momentum transport due to gradients in heat flux in the presence of collisions—through direct solution of the plasma kinetic equations and confirmed through PIC simulations. The results were calculated directly using the finite-difference method of Epperlein and Haines and showed to give valid results. We have tabulated the resulting transport coefficients in a form similar to Braginskii's for ease of use. The results should be relatively easily applied to fluid simulation as a new closure term.

The heat flux viscosity couples to the magnetic fields via the generalized Ohm's law and therefore may play a role in its dynamics. This might be observed in high-energy-density regimes where the magnetic fields can be expected to be advected by a strong heat flux which dominates over ordinary plasma flows. Heat flux viscosity can possibly play an important role in narrow current layers formed in shocks or in magnetic reconnection current sheets and may provide the relevant dissipation for magnetic field line reconnection to occur. In a subsequent paper (written in collaboration with the University of Michigan group), we will apply the present results to recent numerical simulations of Nernst reconnection in a HED plasma[12].

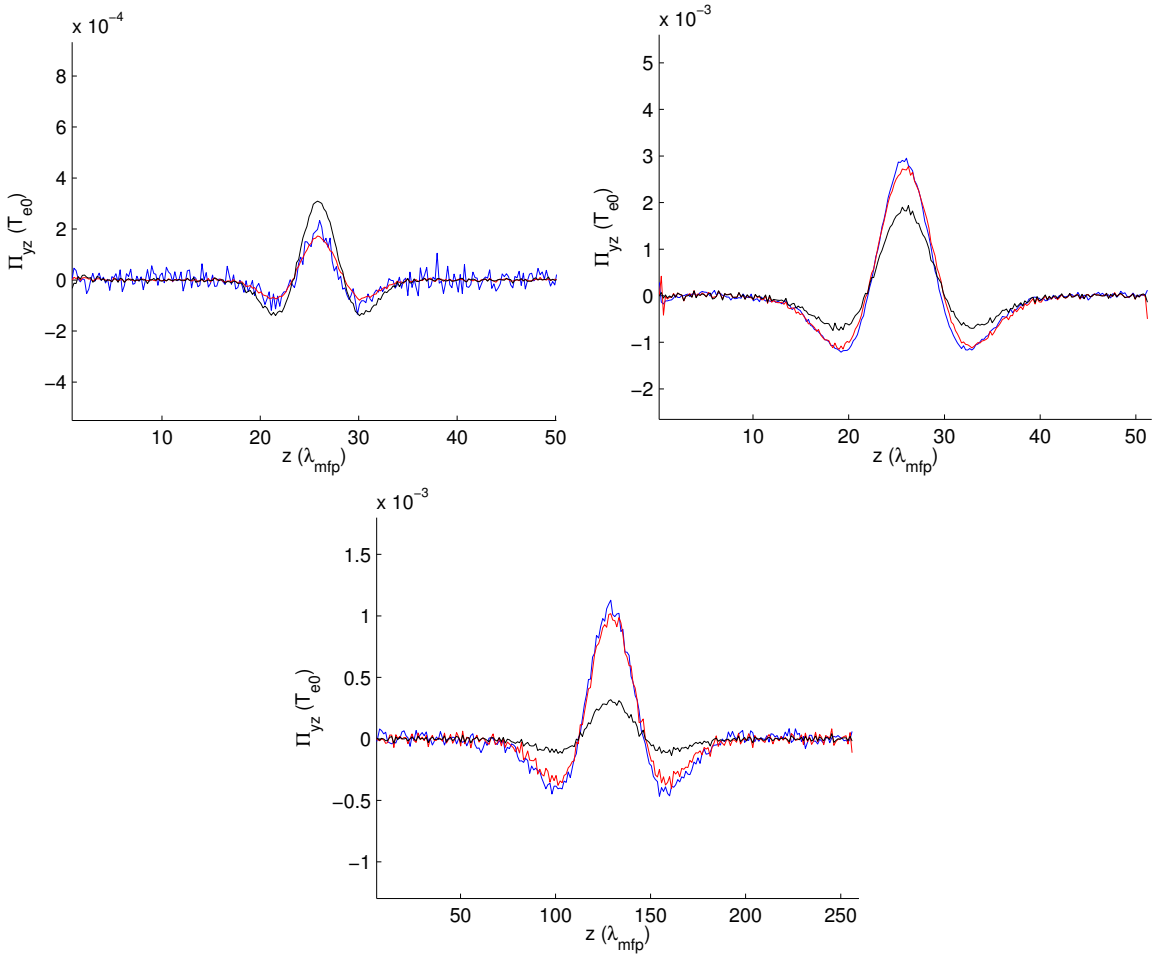

FIG. 4. Results of the anisotropic pressure component Π_{yz} for $\Omega_e\tau = 5, 1, 0.2$. Blue line is the PIC simulation result. Red line is the result from Eq. (22, 25). Black line is the result of LPE2.

ACKNOWLEDGMENTS

We thank A. S. Joglekar, A. G. R. Thomas, and J.-Y. Ji for very helpful discussions. The PIC simulations were conducted on the Kraken supercomputer from the Extreme Science and Engineering Discovery Environment (XSEDE), which is supported by National Science Foundation grant number ACI-1053575, and the Hopper supercomputer from the National Energy Research Scientific Computing Center, a DOE Office of Science User Facility supported by the U.S. Department of Energy under Contract No. DE-AC02-05CH11231. This work is supported by the U.S. Department of Energy under Contract DE-SC0008655.

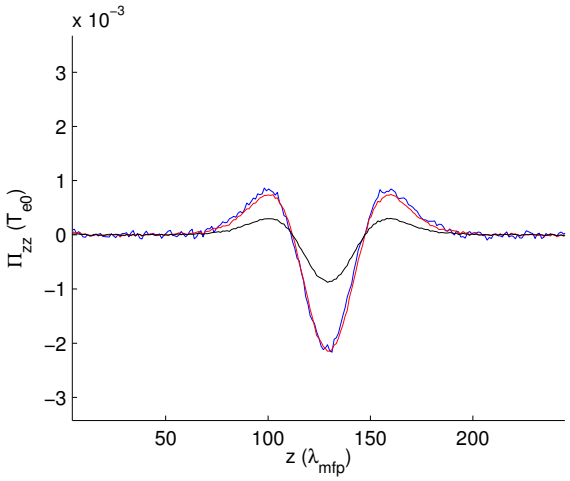

FIG. 5. Results of the anisotropic pressure component Π_{zz} for no magnetic field and $\tau = 3/\omega_{pe}$. Blue line is the PIC simulation result. Red line is the result from Eq. (22, 25). Black line is the result of LPE2.

REFERENCES

[1]P. Y. Chang, G. Fiksel, M. Hohenberger, J. P. Knauer, R. Betti, F. J. Marshall, D. D. Meyerhofer, F. H. Sguin, and R. D. Petrasso, Phys. Rev. Lett. **107**, 035006 (2011).

[2]J. R. Rygg, F. H. Sguin, C. K. Li, J. A. Frenje, M. J.-E. Manuel, R. D. Petrasso, R. Betti, J. A. Delettrez, O. V. Gotchev, J. P. Knauer, D. D. Meyerhofer, F. J. Marshall, C. Stoeckl, and W. Theobald, Science **319**, 1223 (2008).

[3]S. H. Glenzer, W. E. Alley, K. G. Estabrook, J. S. D. Groot, M. G. Haines, J. H. Hammer, J.-P. Jadaud, B. J. MacGowan, J. D. Moody, W. Rozmus, L. J. Suter, T. L. Weiland, and E. A. Williams, Phys. Plasmas **6**, 2117 (1999).

[4]M. G. Haines, Plasma Phys. Control. Fusion **28**, 1705 (1986).

[5]A. Nishiguchi, T. Yabe, M. G. Haines, M. Psimopoulos, and H. Takewaki, Phys. Rev. Lett. **53**, 262 (1984).

[6]A. Nishiguchi, T. Yabe, and M. G. Haines, Phys. Fluids **28**, 3683 (1985).

[7]A. Hata, K. Mima, A. Sunahara, H. Nagatomo, and A. Nishiguchi, Plasma Fusion Res. **1**, 020 (2006).

[8]H. Nagatomo, T. Johzaki, A. Sunahara, H. Sakagami, K. Mima, H. Shiraga, and H. Azechi, Nucl. Fusion **53**, 063018 (2013).

[9]L. Willingale, A. G. R. Thomas, P. M. Nilson, M. C. Kaluza, S. Bandyopadhyay, A. E.

Dangor, R. G. Evans, P. Fernandes, M. G. Haines, C. Kamperidis, R. J. Kingham, S. Minardi, M. Notley, C. P. Ridgers, W. Rozmus, M. Sherlock, M. Tatarakis, M. S. Wei, Z. Najmudin, and K. Krushelnick, Phys. Rev. Lett. **105**, 095001 (2010).

[10]C. P. Ridgers, R. J. Kingham, and A. G. R. Thomas, Phys. Rev. Lett. **100**, 075003 (2008).

[11]B. Dubroca, M. Tchong, P. Charrier, V. T. Tikhonchuk, and J.-P. Morreeuw, Phys. Plasmas **11**, 3830 (2004).

[12]A. Joglekar, A. Thomas, W. Fox, and A. Bhattacharjee, Phys. Rev. Lett. **112**, 105004 (2014).

[13]E. Priest and T. Forbes, *Magnetic Reconnection* (Cambridge University Press, 2000).

[14]M. Hesse and D. Winske, J. Geophys. Res. **103**, 26479 (1998).

[15]A. Divin, S. Markidis, G. Lapenta, V. S. Semenov, N. V. Erkaev, and H. K. Biernat, Phys. Plasmas **17**, 122102 (2010).

[16]Y.-M. Huang, A. Bhattacharjee, and T. G. Forbes, Phys. Plasmas **20**, 082131 (2013).

[17]E. M. Epperlein and M. G. Haines, Phys. Fluids **29**, 1029 (1986).

[18]S. I. Braginskii, Rev. Plasma Phys. **1**, 205 (1965).

[19]R. Herdan and B. S. Liley, Rev. Mod. Phys. **32**, 731 (1960).

[20]E. M. Epperlein, J. Phys. D: Appl. Phys. **17**, 1823 (1984).

[21]J.-Y. Ji and E. D. Held, Phys. Plasmas **20**, 042114 (2013).

[22]I. P. Shkarofsky, Can. J. Phys. **41**, 1753 (1963).

[23]I. P. Shkarofsky, T. W. Johnston, and M. P. Bachynski, *The Particle Kinetics of Plasmas* (Addison-Wesley, 1966).

[24]K. Germaschewski, W. Fox, N. Ahmadi, L. Wang, S. Abbott, H. Ruhl, and A. Bhattacharjee, arXiv:1310.7866 [physics] (2013), arXiv: 1310.7866.

PPPL PRINCETON PLASMA PHYSICS LABORATORY

Princeton Plasma Physics Laboratory
Office of Reports and Publications

Managed by
Princeton University

under contract with the
U.S. Department of Energy
(DE-AC02-09CH11466)

P.O. Box 451, Princeton, NJ 08543
Phone: 609-243-2245
Fax: 609-243-2751

E-mail: publications@pppl.gov

Website: http://www.pppl.gov